2010 Conference on Control and Fault Tolerant Systems
Nice, France, October 6-8, 2010

DTFC versus MPC for induction motor control reconfiguration after inverter faults

Matías A. Nacusse Mónica Romero Hernan Haimovich María M. Seron

Abstract— **This work compares the use of direct torque and flux control (DTFC) and model predictive control (MPC) for induction motor (IM) control. These two strategies are fundamentally different in operation since (i) DTFC decides the current control action based on a switching table constructed using a simplified model of the IM, whereas (ii) MPC decides the current control action by on-line minimization of a cost function that uses the available inverter output voltages as optimization variables. Emphasis is given in this work to the reconfiguration of the control action after voltage source inverter faults. We assume that the fault can be suitably detected and isolated and that the inverter can be reconfigured after the specific fault to continue operation, albeit with a reduced set of achievable output vectors. Based on this reduced set of vectors, we propose to reconfigure the induction motor control algorithm by (i) instructing DTFC to use a *reconfigured switching table* or (ii) providing the reduced set of inverter vectors as the *reconfigured constraint set* of optimization variables for MPC. Simulation results show that MPC considerably outperforms DTFC at a modest increment of computational cost. Moreover, this increment is less pronounced under fault since the number of optimization variables is reduced.**

Keywords: **fault tolerant control, direct torque and flux control, model predictive control, induction motor, inverter faults.**

I. INTRODUCTION

Direct torque and flux control control (DTFC) is a vector control strategy that directly controls the stator flux magnitude and the electromagnetic torque of an induction motor (IM). In this strategy, the control actions are chosen directly from a so-called *switching table*. The switching table (ST) is constructed taking into account the desired action on flux and torque (i.e., to increment or to decrement) and the position of the stator flux vector [1][2]. The control actions are three-phase voltages provided by a voltage source inverter (VSI) (see Fig. 1), which can be represented as voltage vectors in a stationary frame of reference, the so-called *(a,b)*-plane. Under normal (healthy) operation, there are eight possible vectors, depending on the switch configurations, where six of them are called active vectors and two are null vectors since they produce null line voltage (see Fig. 2).

M. Nacusse and H. Haimovich are with CONICET and Departamento de Control, Facultad de Ciencias Exactad Ingeniería y Agrimensura, Universidad Nacional de Rosario, Argentina. {nacusse,haimo}@fceia.unr.edu.ar

M. Romero is with Departamento de Electrónica, Facultad de Ciencias Exactad Ingeniería y Agrimensura, Universidad Nacional de Rosario, Argentina. mromero@fceia.unr.edu.ar

M.M. Seron is with the Centre for Complex Dynamic Systems and Control, the University of Newcastle, Australia . maria.seron@newcastle.edu.au

This work has been partially supported by the Agencia Nacional de Promoción Científica y Tecnológica, Argentina, under project PICT 2008-0650 (FONCyT).

The ST can be considered as a result of a *prediction* procedure where, using a reduced model of an IM, we predict its behavior when different voltage vectors are applied, according to the position of the stator flux. However, the selection of the appropriate vector to apply, based on this prediction and the desired action on flux and torque, follows heuristic reasoning. This suggests the possibility to improve performance by resorting to some type of optimization [3]. In this work we thus propose to select the control actions by means of model predictive control (MPC) [4], [5], which minimizes an optimization criterion (cost function) based on some model outputs predicted over a time period (the *prediction horizon*) using a model of the IM. Specifically, in the current paper we utilize a cost function which weights the square of the errors between predicted flux magnitude and torque, and their respective desired references. The optimization variables used by MPC are the *(a,b)*-components of the stator voltage vector, taking into account that only eight (healthy operation) or fewer (faulty operation) voltage vectors can be produced by the VSI.

In certain implementations of IM control, where continuous operation of the system must be ensured, the use of a fault tolerant inverter is desirable to avoid the need for parallel redundancy. There are many different fault tolerant topologies for an AC motor drive. Here we use the switch redundant topology discussed in [6], [7] and [8]. We consider two kinds of faults that can be handled by this topology: a short-circuit fault of one switch device and an open-circuit fault. We assume that a fault detection and isolation algorithm detects which component is in faulty condition and performs the necessary actions in order to reconfigure the inverter. After this reconfiguration process, the inverter can generate only four voltage vectors, according to the switch combinations available after a fault occurrence, instead of the eight voltage vectors obtained in healthy operation conditions. Based on this reduced set of vectors, we propose to reconfigure the induction motor control algorithm in the following ways depending on which strategy, DTFC or MPC, is employed:

- instructing DTFC to use a *reconfigured switching table* proposed in [9], or
- providing the reduced set of inverter vectors as the *reconfigured constraint set* of optimization variables for MPC.

Simulation results show that MPC considerably outperforms DTFC at a modest increment of computational cost. Moreover, this increment is less pronounced under fault since the

number of optimization variables is reduced. In addition, the voltage vectors applied by the MPC strategy are compared with those applied by the DTFC strategy in order to analize the switching losses in the VSI.

The remainder of the paper is organized as follows. In Section II the fault tolerant voltage source inverter [7] is reviewed. In Section III some concepts of the DTFC strategy [9] are presented and a reconfigured DTFC (ReDTFC) strategy is proposed to handle faults in the VSI. In Section IV the MPC approach for IM control is presented and a reconfigured MPC (ReMPC) strategy is proposed. In Section V, some simulation results are shown in order to demonstrate the continuous operation of the system as well as its good dynamic response. Section VI presents conclusions and discusses future work.

II. Fault Tolerant Inverter

As mentioned in the previous section, the IM is fed by a VSI which provides eight voltage vectors depending on the state of the switches S_1, S_2 and S_3, corresponding to phases R, S and T, respectively, see Figs. 1, 2. The voltages V_{sR}, V_{sS} and V_{sT} represent the stator phase voltages of the IM and V_{DC} is the voltage of the DC bus. There are many different fault tolerant topologies for an AC motor drive. Here we employ a switch redundant topology presented in [6], [7] and [8]. The schematic circuit is depicted in Fig. 3. This topology incorporates four Triacs (TR_R, TR_S, TR_T and TR_n) and three fast acting fuses (Fs_R, Fs_S, and Fs_T) that provide a good fault tolerant capability and low cost, due to the small number of electronics components added [6]. The switch redundant topology can handle three different kinds of fault: a short-circuit fault of one switch device, an open-circuit fault of one switch device and a single phase open-circuit. Here we focus on the first two types of faults.

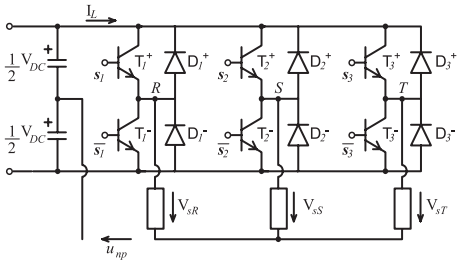

Fig. 1. Schematic circuit of a standard VSI

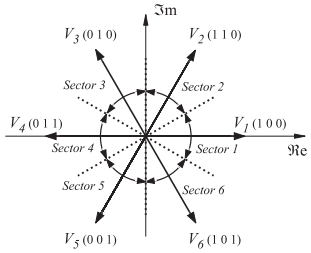

Fig. 2. Voltage vectors and sectors

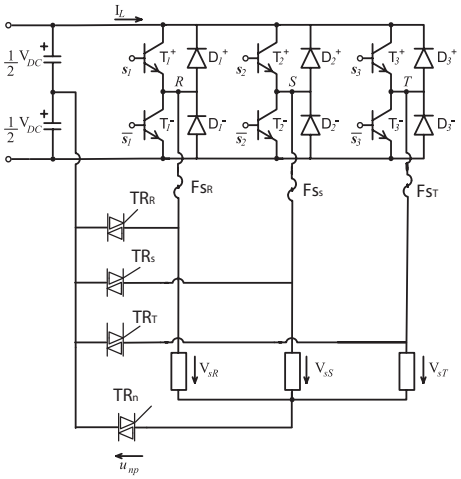

Fig. 3. Schematic circuit of a switch redundant fault tolerant inverter

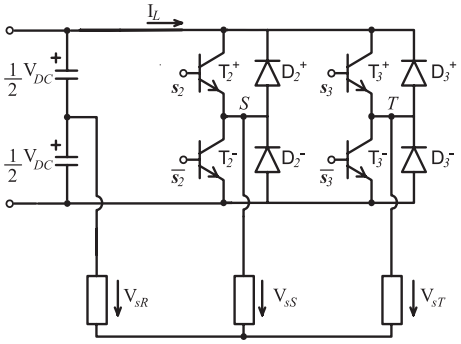

Fig. 4. Schematic circuit after fault in the R Branch

When a short-circuit switch fault is detected, for example in phase R, the TR_R is triggered and the fuse Fs_R opens due to the resulting high current. The resulting inverter configuration is represented in Fig. 4. We assume that a fault detection and isolation algorithm diagnoses which component is in faulty condition and performs the triggers required to isolate the fault. After this reconfiguration process, the inverter can generate only four voltage vectors, according to the available switch combinations, instead of the eight voltage vectors obtained in healthy operation conditions. The new voltage vectors are different depending on which branch is faulty. Equations (1) represent the output voltages of the VSI in terms of the switch states S_i (with $i = 1,2,3$).

$$\begin{aligned} V_R &= \frac{V_{DC}}{3}(2S_1 - S_2 - S_3) \\ V_S &= \frac{V_{DC}}{3}(2S_2 - S_3 - S_1) \\ V_T &= \frac{V_{DC}}{3}(2S_3 - S_1 - S_2) \end{aligned} \tag{1}$$

In absence of failure the S_i can take the values 0 or 1, depending on whether the lower switch or the upper switch of each branch is in conduction, respectively. After reconfiguration due to fault, a phase terminal of the stator is connected to the middle point of the DC bus. The corresponding output voltage of the VSI for that branch can be represented by

an "under-fault" switch value $S_i^F = 0.5$. For example, after reconfiguration due to a fault in the R branch the output voltages of the inverter are:

$$\begin{aligned} V_R &= \frac{V_{DC}}{3}(1 - S_2 - S_3) \\ V_S &= \frac{V_{DC}}{3}(2S_2 - S_3 - 0.5) \\ V_T &= \frac{V_{DC}}{3}(2S_3 - S_2 - 0.5) \end{aligned} \tag{2}$$

The voltage vectors possible after fault reconfiguration are shown in Fig. 5 in the stationary reference frame (a,b) for faults in the R, S, or T branches. Notice that the first harmonic amplitude of the new VSI configuration, represented by the maximum circumference inscribed in the diamond determined by the new voltage vectors, is half the amplitude of that given by the healthy VSI. This loss of voltage capabilities produces loss of performance of the induction motor, i.e., the motor has to shift to field weakening operation at half rated speed for rated load.

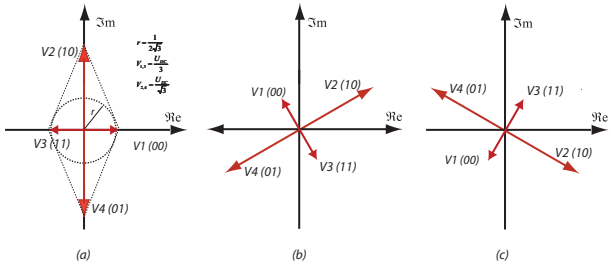

Fig. 5. Voltage vectors for a fault in: (a) R, (b) S, (c) T branch

III. Direct Torque and Flux Control

This section gives a brief description of the principles of the standard DTFC scheme [1][2] and presents a reconfigured DTFC strategy in order to maintain the system operability after a fault occurrence.

A. Classical DTFC strategy

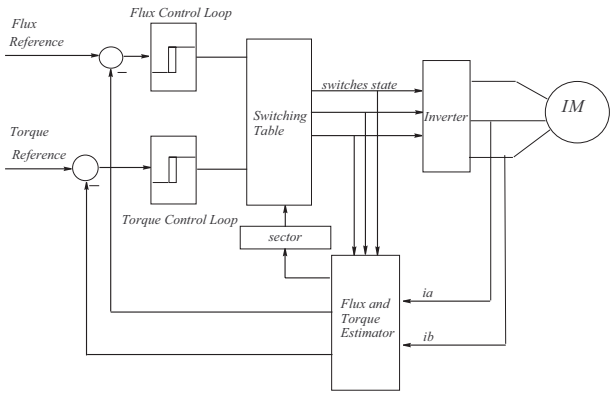

Fig. 6. Schematic of stator flux based DTFC induction motor drive with VSI

DTFC is a vector control strategy that directly controls the stator flux magnitude and the electromagnetic torque of an induction motor. The strategy consists of two control loops, associated to the stator flux magnitude and to the electromagnetic torque, respectively. Each control loop has a hysteresis comparator that indicates which control action must be performed (to increment or to decrement the magnitudes of stator flux and torque). A switching table is constructed so that, given the current flux vector position and the desired control actions, the appropriate voltage vector to be applied to the motor can be selected.

The DTFC control strategy is based on the dynamic equations of the stator flux and electromagnetic torque. The dynamics of the stator flux vector, $\overline{\lambda_s}$, are given by

$$\dot{\overline{\lambda_s}} = \overline{V_s} - \overline{i_s} R_s, \tag{3}$$

where $\overline{V_s}$ is a voltage vector, $\overline{i_s}$ is the stator current vector and R_s is the stator resistance. The standard DTFC strategy assumes that the voltage drop on the stator resistance R_s can be neglected and hence the dynamics of the stator flux are only governed by $\overline{V_s}$. Therefore, application of a specific voltage vector $\overline{V_s}$ during a time interval ΔT yields

$$\overline{\Delta\lambda_s} = \overline{V_s}\Delta T, \tag{4}$$

which shows precisely how the voltage vector affects the stator flux.

The expression of the electromagnetic torque in terms of the stator and rotor flux vectors is

$$\tau_{em} = \frac{3}{2} n_p \frac{L_m}{\sigma L_s L_r} \left|\overline{\lambda_s}\right| \left|\overline{\lambda_r}\right| \sin(\delta), \tag{5}$$

where n_p is the number of pair of poles of the induction machine, L_s and L_r are the stator and rotor inductance, L_m is the magnetization inductance, δ is the angle between rotor and stator flux vectors and σ is the total leakage factor. The rotor flux is known to have a dynamic response slower than that of the stator flux. Hence, provided the time period ΔT is small enough, classical DTFC assumes that the rotor flux is constant with respect to variations in the stator flux. From (5), if the magnitude of the stator flux is maintained constant, then the instantaneous electromagnetic torque is controlled by modifying the angle δ. Thus, to perform the control action, an adequate stator voltage vector must be applied to the induction motor in order to keep the stator flux magnitude constant and make the stator flux rotate to a desired position δ. The standard DTFC algorithm defines six sectors in the stationary reference frame (a,b), where each voltage vector bisects the sector, see Fig. 2, [2] [1]. According to the position of the stator flux vector in relation to this quantification of the complex (a,b)-plane, a suitable voltage switching table is defined [1]. Note that, in classical DTFC, the selection of the appropriate voltage vector to be applied relies only on the estimated stator flux vector and electromagnetic torque, and the desired torque and flux magnitude references (see Fig. 6).

B. Reconfigured DTFC strategy

A reconfigured DTFC (ReDTFC) strategy was presented in [10] where four sectors were defined according to the four

TABLE I

VOLTAGE VECTOR SWITCHING TABLE

τ_{em}	λ_s	$S1$	$S2$	$S3$	$S4$	$S5$	$S6$	$S7$	$S8$
0	0	V_3	V_4	V_4	V_1	V_1	V_2	V_2	V_3
0	1	V_1	V_1	V_2	V_2	V_3	V_3	V_4	V_4
1	0	V_2	V_3	V_3	V_4	V_4	V_1	V_1	V_2
1	1	V_2	V_2	V_3	V_3	V_4	V_4	V_1	V_1

resulting voltage vectors for a fault in the branch of the VSI. Here we employ an improved ReDTFC, proposed in [9], which uses a new quantification of the flux vector position taking into account the contribution of each resulting voltage vector along the whole previous sector. This new ReDTFC reduces the torque ripple and maintains the dynamic response achieved in [10]. Fig. 7 shows the new quantification using eight sectors and, based on them, a new ST is constructed as shown in Table I.

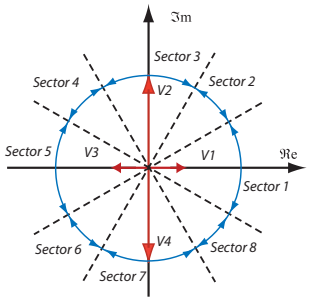

Fig. 7. Sector quantification in (a,b) stationary reference frame for a fault in branch R

The resulting switching table works as follows: in sector 1, V_2 is applied in order to increase torque, V_1 is applied to decrease torque and increase flux, and V_3 is applied to decrease torque and flux. V_4 is never applied in sector 1 because it has a large magnitude and the torque reduction will be too drastic. In sectors 3, 5 and 7 the vectors are chosen following the same reasoning as above. For sector 2 the application of the voltage vector V_2 produces an increase in the flux magnitude and torque; the application of V_1 increases the flux magnitude and decreases torque; V_4 and V_3 produce the opposite effect, respectively. A similar reasoning is used for sectors 4, 6 and 8.

IV. MPC FOR INDUCTION MOTOR CONTROL

Model predictive control (MPC) is a control method that, at each sampling instant, computes the control input to be applied at such instant by solving an open-loop optimal control problem. The initial state for the optimization is taken to be the current system state, and future states are predicted over the prediction horizon using a model of the system. The optimal control sequence resulting from the optimization is an open loop strategy comprising a set of successive control inputs to be applied over the prediction horizon. However, this is converted into a feedback strategy by applying only the first control action of this set and then repeating the whole procedure at the next sampling instant when new measurements of the system states are obtained. This technique is known as receding-horizon control (RHC).

Here we propose to use an MPC strategy for IM control [4], [5], [12]. The full state-space model of the IM can be written as follows:

$$\dot{x}(t) = A_c(\omega(t))x(t) + B_c u(t), \tag{6}$$

$$\dot{\omega} = \mu(\lambda_{ra} i_{sb} - \lambda_{rb} i_{sa}) - \frac{b}{J}\omega - \frac{1}{J}\tau_c, \tag{7}$$

with $x = \begin{bmatrix} i_{sa} & i_{sb} & \lambda_{ra} & \lambda_{rb} \end{bmatrix}^T$, i_{sa}, i_{sb} and λ_{ra}, λ_{rb} are the (a,b) components of the stator current and the rotor flux, respectively, ω is the rotor speed, $u = \begin{bmatrix} V_a & V_b \end{bmatrix}^T$, V_a and V_b the (a,b) components of the applied stator voltage, and where

$$A_c(\omega) = \begin{bmatrix} -\gamma & 0 & \alpha\beta & n_p\beta\omega \\ 0 & -\gamma & -n_p\beta\omega & \alpha\beta \\ \alpha L_m & 0 & -\alpha & -n_p\omega \\ 0 & \alpha L_m & n_p\omega & -\alpha \end{bmatrix}, \quad B_c = \begin{bmatrix} \frac{1}{\sigma L_s} & 0 \\ 0 & \frac{1}{\sigma L_s} \\ 0 & 0 \\ 0 & 0 \end{bmatrix}, \tag{8}$$

with model parameters $\alpha = \frac{R_r}{L_r} = \frac{1}{T_r}$, $\beta = \frac{L_m}{\sigma L_s L_r}$, $\gamma = \frac{1}{\sigma}(\frac{1-\sigma}{T_r} + \frac{1}{T_s})$, $T_s = \frac{R_s}{L_s}$, $\sigma = 1 - \frac{L_m^2}{L_s L_r}$, $\mu = n_p \frac{L_m}{J L_r}$, where R_r is the three-phase rotoric resistance.

Let t_k, for $k = 0, 1, \ldots$ denote the sampling instants and let a subscript k on a variable denote the value of such variable at the corresponding sampling instant, e.g., $x_k = x(t_k)$. Assuming that rotor speed is known and remains approximately constant between sampling instants, an exact discrete-time model equivalent to the continuous-time equations (6) can be found as follows:

$$x_{k+1} = A_k x_k + B_k u_k, \tag{9}$$

where the matrices A_k and B_k are given by (see [12] for further details on the online computation of these matrices)

$$A_k = e^{A_c(\omega_k)\cdot(t_{k+1}-t_k)}, \quad B_k = \int_{t_k}^{t_{k+1}} e^{A_c(\omega_k)\cdot(t_{k+1}-t)} B_c dt. \tag{10}$$

The electromagnetic torque and the squared magnitude of the stator flux are calculated at each sampling time as follows:

$$\begin{aligned} |(\lambda_s)_k|^2 &= [Cx_k]^T [Cx_k] \\ (\tau_{em})_k &= x_k^T T x_k \end{aligned} \tag{11}$$

where the matrices C and T are given by

$$\begin{aligned} C &= \begin{bmatrix} L_s\sigma & 0 & \frac{L_m}{L_r} & 0 \\ 0 & L_s\sigma & 0 & \frac{L_m}{L_r} \end{bmatrix} \\ T &= \frac{3}{2} n_p \frac{L_m}{L_r} \begin{bmatrix} 0 & 0 & 0 & -0.5 \\ 0 & 0 & 0.5 & 0 \\ 0 & 0.5 & 0 & 0 \\ -0.5 & 0 & 0 & 0 \end{bmatrix} \end{aligned} \tag{12}$$

The cost function for the MPC on-line minimization is

$$J = \sum_{\ell=k}^{\ell=k+N} \left\{ W_\tau [\tau_{em}(t_\ell) - \tau_{ref}(t_\ell)]^2 + W_\lambda [|\lambda_s(t_\ell)|^2 - \lambda_{ref}^2(t_\ell)]^2 \right\} \tag{13}$$

where N is the prediction horizon, τ_{ref} and λ_{ref} are the desired reference signals for torque and flux magnitude, respectively, and W_τ, W_λ are weights on each error.

To evaluate the predicted values of torque and stator flux magnitude, $\tau_{em}(t_\ell)$ and $|\lambda_s(t_\ell)|$, for $\ell = k+1,\ldots,k+N$, the model (9)–(11) is used, where rotor speed $\omega(t)$ is assumed to remain constant and equal to $\omega(t_k) = \omega_k$ over the prediction horizon (t_k to t_{k+N}), and the input u_ℓ, for every ℓ, is constrained (in healthy operation) to the finite set consisting of the seven voltage vectors generated by the inverter (since two of the voltage vectors produce null line voltages, the eight possibilities produce only seven different three-phase voltages). Thus, there is a total of 7^N possible sequences of input vectors, and the same number of predicted values for the cost function (13), of which the minimum is selected. The minimizing sequence consists of N voltage vectors. The first vector of this sequence is applied and a new sequence is recalculated at the next sampling time.

A. Reconfigured MPC strategy

As explained in Section II, there are only 4 vectors after a reconfiguration of the VSI. Hence, it is possible to reconfigure the MPC control algorithm using the same cost function but constraining the input to the finite set consisting of the new, "after-fault", voltage vectors. Notice that in this case the number of possible control input sequences over the prediction horizon is reduced to 4^N.

V. Simulation Results

In this section, simulation results are presented in order to compare the performances of DTFC and MPC and their associated reconfiguration strategies, ReDTFC and ReMPC, respectively. In particular, for the MPC strategy we consider two values of the prediction horizon in the cost function (13), namely, $N = 1$ (noted MPC1 and ReMPC1) and $N = 2$ (noted MPC2 and ReMPC2). The simulations were performed using Matlab/Simulink with the toolbox developed in [11], and the power electronics components are modeled as ideal switches. A cascaded control structure for speed control is employed, adding a PI controller to compute the desired torque reference. The stator currents and the rotor speed are measured and the respective fluxes are estimated.

The induction motor chosen for simulation has the following parameters: $R_r = 0.39923\Omega$, $R_s = 1.165\Omega$, $J = 0.0812Nm$, $L_s = 0.13995Hy$, $L_r = 0.13995Hy$, $L_m = 0.13421Hy$, and $n_p = 2$. The PI parameters are $P_w = 7.05$ and $I_w = 0.0282$ and the weights in the cost function (13) are $W_\tau = 0.0091$ and $W_\lambda = 0.09$. The switching sampling period is $T_s = 0.1ms$.

The simulation scenario is as follows. The rotor speed reference is a ramp that starts at time zero with final value $75rad/s$. At time $T = 1s$ a load torque $\tau_l = 24Nm$ is applied. At time $T = 2s$ a fault in the R branch of the fault tolerant VSI occurs. Fig. 8 shows the resulting electromagnetic torque, which has achieved steady state conditions when the fault in the VSI occurs. The associated stator flux magnitude evolution in presence of the fault is shown in Fig. 9. We can observe the improvement achieved with both the ReMPC1 and ReMPC2 strategies with respect to the ReDTFC strategy.

TABLE II
Cost Table

Cost	*ReDTFC*	*ReMPC1*	*ReMPC2*
Healthy	0.8155	0.1102	0.1632
Faulty	0.6737	0.1319	0.2005

Figs. 10 and 11 show the voltage vectors applied in healthy and faulty conditions by the ReMPC1 and ReMPC2 strategies, respectively.

Note that, in healthy operation, both strategies apply voltages that are not allowed in DTFC [2] for a given sector; for example, in sector 1, DTFC applies only vectors V_2, V_3 and V_0 or V_7, while MPC1 and MPC2 also applies V_1 and V_4. These control actions are responsible for the torque ripple reduction but they involve a greater number of commutations of the inverter switches, which produce associated commutation losses. In faulty condition, both ReMPC strategies, apply voltage vectors in a similar way because the VSI can only produce 4 different voltage vectors.

Another characteristic that we observe in the simulated torque response is that the faulty ripple amplitude is smaller than the healthy one. This is because the magnitude of the reconfigured voltage vectors are smaller than the original ones i.e., for the healthy VSI the magnitude of the voltage vectors is $\frac{2}{3}V_{DC}$ whereas for the reconfigured VSI the maximum magnitude of a voltage vector is $\frac{1}{\sqrt{3}}V_{DC}$.

Table II shows the cost function calculated over 1000 points (0.1 seconds) obtained from simulation tests of ReDTFC and ReMPC, for both healthy and faulty conditions. All tests were performed in steady state regime. Note that the lowest cost values correspond to MPC with $N = 1$ in all the operating conditions simulated. This perhaps surprising result could be caused by the fact that the sequence of two voltage vectors selected by the ReMPC strategy optimizes the cost function, but the first vector, which is the one applied, produces a weighted torque and flux magnitude ripple greater than that obtained with MPC1. Another possible cause of this result is the assumption that rotor speed remains constant over the prediction horizon which corresponds to 200 μs for $N = 2$.

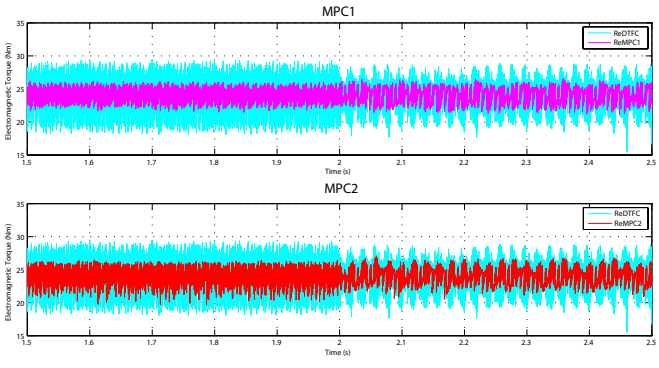

Fig. 8. Electromagnetic torque for ReDTFC (in light blue) and ReMPC

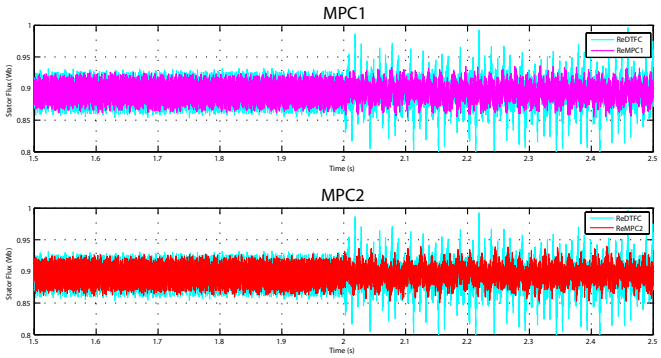

Fig. 9. Stator flux magnitude for ReDTFC (in light blue) and ReMPC

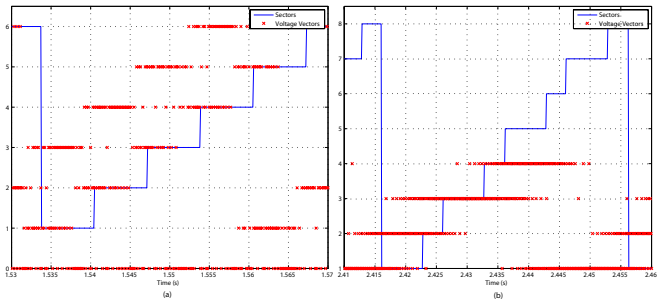

Fig. 10. Voltage vectors applied for ReMPC1. (a) healthy , (b) faulty

VI. CONCLUSIONS

We have presented a reconfigured model predictive control strategy (ReMPC) to reconfigure an induction motor control algorithm after faults in the VSI that feeds the motor. The ReMPC strategy was compared with a reconfigured DTFC strategy (ReDTFC) previously proposed by the first two authors. The simulation results show the achieved improvement of the ReMPC strategy with respect to the ReDTFC strategy. This improvement can be explained by the fact that, in order to select the appropriate input voltage vector, the MPC strategy benefits from knowledge of all the five state variables of the IM model, whereas DTFC employs only two variables: stator flux and electromagnetic torque. In addition, for prediction, MPC utilises a more complete model of the induction motor than that considered by the DTFC strategy. On the other hand, the mentioned improvement involves a greater number of commutations in the VSI. We have also observed that, in steady conditions, ReMPC with prediction horizon $N = 1$ has better performance than ReMPC with $N = 2$, in addition to lower computation cost. The different performance achieved could be due to the fact that, for prediction purposes, rotor speed was assumed to remain constant over the prediction horizon, and this assumption is less likely to be satisfied for larger prediction horizons (greater N).

As future work we propose the possibility to include switch losses associated with commutation in the MPC cost function.

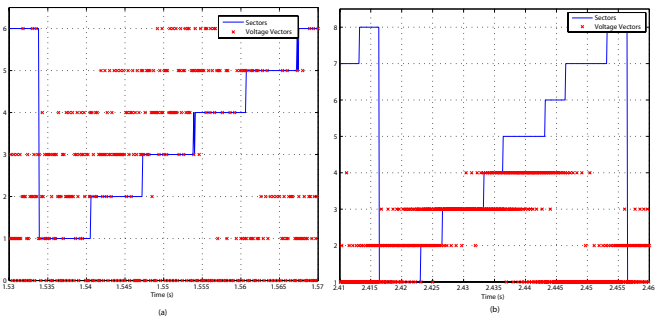

Fig. 11. Voltage vectors applied for ReMPC2. (a) healthy , (b) faulty

REFERENCES

[1] I. Takahashi and T. Noguchi. "A new quick response and high-efficiency control strategy of an induction motor". *IEEE Trans. Industry Appl., 22:820-827*, 1986.

[2] M. Depenbrok. "Direct self-control (dsc) of inverter-fed induction machine". *IEEE Trans. on Power Electronics., 3:420-429*, 1988.

[3] Escobar, G.; Stankovic, A.M.; Galvan, E.; Carrasco, J.M.; Ortega, R., "A family of switching control strategies for the reduction of torque ripple in DTC", *Control Systems Technology, IEEE Transactions on* vol.11, no.6, pp. 933- 939, Nov. 2003

[4] T. Geyer, G. Papafotiou, and M. Morari. "Model Predictive Direct Torque Control—Part I: Concept, Algorithm, and Analysis". *IEEE Trans. Industrial Electronics 56(6):1894-1905*, 2009.

[5] S. Bolognani, S. Bolognani, L. Peretti, and M. Zigliotto. "Design and implementation of Model Predictive Control for electrical motor drives". *IEEE Trans. Industrial Electronics 56(6):1925-1936*, 2009.

[6] A. Welchko, T. A. Lipo, T. M. Jahns, S. E. Schulz, "Fault Tolerant Three-Phase AC Motor Drive Topologies: A Comparison of Features, Cost and Limitations". *IEEE Trans. on Power Electronics, vol. 19, no. 4*, pp. 1108-1116, 2005.

[7] J. R. Fu, T. A. Lipo, "A strategy to isolate the switching device fault of a current regulated motor drive", in *Conf. Rec. IEEE IAS Annu. Meeting, vol. 2*, pp. 1015-1020, 1994.

[8] T. A. Lipo - T. H. Liu - J. R. Fu, "A strategy for improving Reliability of Field-Oriented Controlled Induction Motor Drives". *IEEE Trans. on Industry Applications, vol. 29, no. 5*, pp. 910-918, 1997.

[9] M. Nacusse, M. Romero, S. Junco. "A New Fault Tolerant Direct Torque and Flux Control Strategy with Torque Ripple Reduction". *Technical Report LSD0310 Laboratorio de sistemas dinámicos y procesamiento de la información, Departamento de Control, Facultad de Ciencias Exactad Ingeniería y Agrimensura, Universidad Nacional de Rosario, Argentina. 2010*

[10] Yznaga Blanco Ivonne, Dan Sun, Yi-kang He, "Study on inverter fault-tolerant operation of PMSM DTC". *Journal of Zhejiang University SCIENCE A.Vol.9 No.2*. 2008

[11] F. Felicioni, T. Pérez, H. Molina, S. Junco: "Simudrives: A Tool for Computer-Aided Simulation of Electrical Drives and Motion Control Systems". *XVIII Congreso Argentino Control Automtico, AADECA 2002*, 2-4 Sept. 2002, Buenos Aires, Argentina.

[12] H. Miranda, P. Cortés, J. I. Yuz, and J. Rodríguez. "Predictive torque control of induction machines based on state-space models". *IEEE Trans. Industrial Electronics 56(6):1916-1924*, 2009.